Characterization of liquid crystals impregnated micrometric diffraction gratings for an active near-IR light extraction control

Anatole Héliot, Sylvain Pelloquin, Olivier Gauthier-Lafaye, Antoine
Monmayrant, Henri Camon, T. Gacoin, K. Lahlil, L. Martinelli, C. Biver, S.
Archambeau

Characterization of micrometric diffraction gratings for an active Near-IR light extraction control

A. Héliot✉[123] • S. Pelloquin[1] • O. Gauthier-Lafaye[1] • A. Monmayrant[1] • H. Camon[1] • T. Gacoin[2] • K. Lahlil[2] •
L. Martinelli[2] • C. Biver[3] • S. Archambeau[3]

Abstract

Due to their narrow reflection peak as well as their compact structure, Guided Mode Resonance Filters (GMRFs) are attractive for many applications. We demonstrate the possibility to modulate the properties of a GMRF by associating it with liquid crystals (LCs). By impregnating the diffraction grating with LCs, it is possible to switch between an active and an inactive state depending on the polarization of the light or the applied voltage. In this paper we fabricated and characterized the first diffraction order of LC-impregnated gratings with different periods (0,8 to 5,0µm) and depths (130 to 840nm) to test the ability of liquid crystals to adjust the diffraction properties. Finally, around 99.8% of diffraction intensity turns off with a 90° rotation polarization at zero voltage and 90 to 99% by applying a voltage of 30V according to the grating dimensions. The effect of the grating dimension on the diffraction modulation capacity are discussed.

1 Introduction

Combining a waveguide and a diffractive structure, one can form a GMRF which is particularly effective to produce narrow-band spectral filters. These structures represent a very promising alternative to conventional Fabry-Perot multilayer filters (Wang and Magnusson 1993) and can also be used to directionally couple or extract light confined in the core of a waveguide (Taillaert et al. 2002)

Modulating a GMRF by using an active material has been the subject of considerable interest as such filters are attractive for many applications from optical modulators (Sharon et al. 1996) to tunable lasers (Zheng et al. 2012) due to their simple and compact structure as well as their narrow and sharp reflection peak.

Liquid crystals are of much interest in this purpose as they are the subject of many researches since the seventies and are used at an industrial scale in liquid crystal displays (LCD) screens. More recently, the birefringence of nematic liquid crystals and their mobility under an electric field have enabled the realization of active optical structures.

Many researches have already demonstrated the ability of liquid crystals to modulate the diffraction of a Bragg grating under an electric field. A first approach involves the use of a GMRF with liquid crystals in the cladding layer (Wang et al. 2013). By switching the liquid crystals through the application of an electric field, the effective index of the guided mode evolves leading to a variation of the resonance wavelength of about 20nm (Chang et al. 2007).

In a second approach, the LC layer is used to create a diffraction grating due to a periodic orientation of the molecules. For example, a network of interdigitated electrodes allows to periodically align the molecules when an electric field is applied, constituting a diffraction grating (Lindquist et al. 1994; Gao et al. 2016). Another approach is to form a diffraction grating through a structured alignment of the molecules by micro-friction (Wen et al. 2002) or by photo-alignment (Kaspoutine et al. 2006; Lu et al. 2006; Hu et al. 2012). The resulting diffraction is annihilated when an electric field is applied forming a uniform homeotropic alignment. Finally, the dispersion of liquid crystals in a polymer subjected to light interference can form holographic polymer dispersed liquid crystal (HPDLC). The holographic pattern fixes the LCs in place by polymerization, while the non-insulated parts are still mobile while the other part is still mobile. The resulting diffraction grating is electrically switchable (Margerum et al. 1992; Pavani et al. 2009; Caputo et al. 2004).

The purpose of the study presented here is to directly modulate the diffraction intensity of a grating to create an active GMRF in the near-infrared (NIR) range. For this, it is necessary to use a grating with a period in the micron range

✉ A. Héliot
    anatole@heliot.com

[1] LAAS-CNRS, Université de Toulouse, CNRS,
    Toulouse, France
[2] Laboratoire PMC, UMR 7643, Ecole Polytechnique, CNRS,
    Palaiseau, France
[3] ESSILOR International, Labège, France

(Alonso-Ramos et al. 2012). Previous approaches do not meet this criterion because they either modulated slightly the filtered wavelength or have a limited effect when the grating period is in the micron range.

2 Principle and implementation

2.1 Principle

The idea developed here is to impregnate a GMRF with liquid crystals whose ordinary index (n_o) is of the same order than the refractive index of the grating (n_g). Thus, by switching the liquid crystals inside the diffraction grating by applying an electric field, it is *a priori* possible to modulate directly the Δn of the structure from a high Δn (n_e-n_g) inducing a strong diffraction to a negligible Δn (n_o-n_g) switching the diffraction off. The principle is the same considering a diffraction grating used in transmission (Fig. 1). However, if it is necessary to use a micrometric grating to extract Near-IR light, these dimensions allow to diffract the visible light in transmission (Chen et al. 2017).
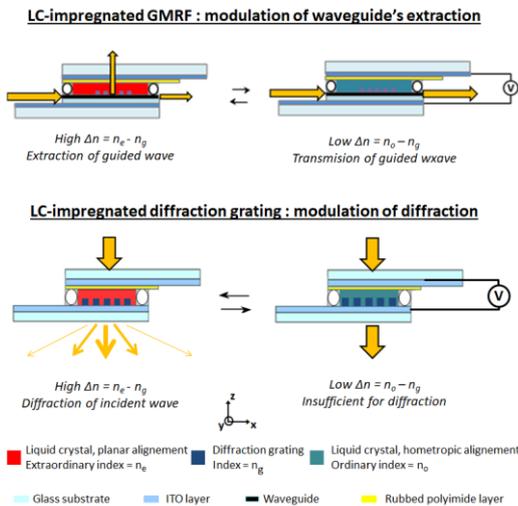

Fig. 1. Schematic view of the principle of modulation of waveguide's extraction by LC-impregnated GMRF (above) and modulation of diffraction by LC-impregnated grating (below). In both cases, the diffractive state ($\Delta n=n_e-n_g$) is represented in left and the non-diffractive state ($\Delta n=n_o-n_g$) in right.

2.2 Problematic

In order to validate this principle, liquid crystal cells with diffraction gratings have been prepared and characterized in transmission with a normal incident visible light. The characterization in transmission allows to isolate the diffraction grating of the waveguide and thus to focus essentially on the interaction between the diffraction grating and the liquid crystals. The objective is to answer the following questions:

- What is the alignment of liquid crystals in the diffraction gratings?
- Does the mobility of liquid crystals confined in micronic or sub-micronic structures allow to significantly modulate the diffraction?
- What is the effect of the grating dimensions (period, depth) on the mobility of molecules and is there a limit?

2.3 Materials and implementation

Different diffraction gratings were realized on glass wafer (AF32, Schott) previously covered by ITO (Solems). The structures are formed on curable resins which refractive index is around 1,52 at 635nm. Depending on the dimensions, two processes were used.

- For grating with periods superior to 1µm, projection photolithography process has been used. An organic-inorganic hybrid resin (ULIS, Essilor (Biver et al. 2009)) is used with stepper (Canon 3000i4).
- For periods inferior to 1µm, nanoimprint lithography (NIL) was carried out. A home-made resin (NILUV, (Doucet et al. 2016)) is used for soft mold NIL process (Pelloquin et al. 2018).

Gratings with depths ranging from 120 to 840nm and with periods from 0.8 to 5.0µm are realized. Filling factors of diffraction gratings are 0.5 and we can therefore consider grooves of 0.4 to 2.5µm of width (Fig. 2).

7µm thick cells were then formed by assembling the structures made with another glass plate, previously covered by ITO and rubbed polyimide (SUNEVER 5291, Nissan Chemical Industries). Cells are then filled with liquid crystals E7 ($n_o=1.52$; $n_e=1.73$ at 25°C, EM Industries Inc) or refractive index liquid (Cargill) as references.
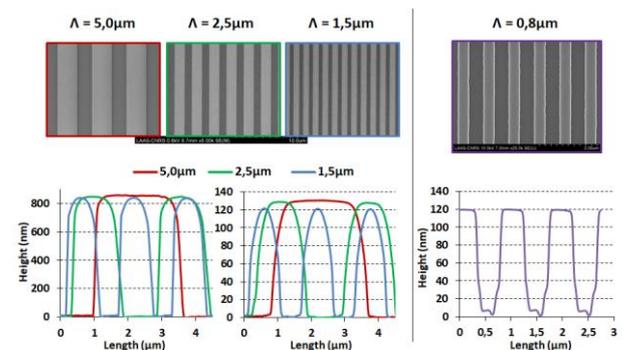

Fig. 2. SEM images (upper part) and AFM characterizations (lower part) of gratings from 0.8 to 5.0µm fabricated by photolithography (left) or by nano-imprint lithography (right).

2.4 Definition of different cases according to the polarization and LC's alignment

Experiments were carried out with an incident light perpendicular to the surface. Four different cases can be distinguished depending on the polarization of the incident light and the application of an electric field (Fig. 3).
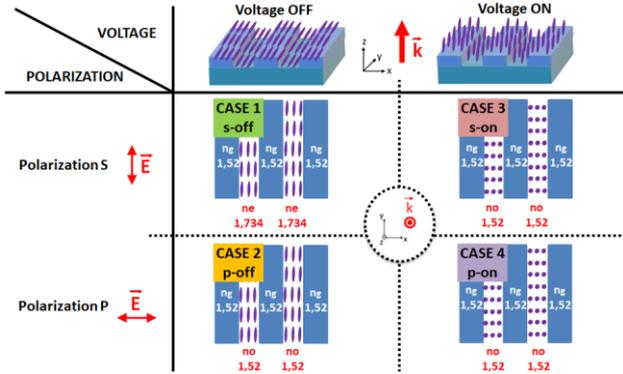

Fig. 3. Scheme of the different situations according to the incident polarization and the applied voltage governing the LC orientation.

One can notice that only the CASE1 induces a high Δn theoretically triggering the diffracting state.

3 Monochromatic characterization

These different cases will be characterized with a monochromatic incident beam, at 635 nm, and with a white source to study the influence of wavelength.

3.1 Modulation of incident polarization without tension (comparison of CASE1 and CASE2)

CASE1 and CASE2 have been first compared with various cells filled with isotropic liquids of different refractive indexes. Measured diffraction for 840nm depth was then compared to RCWA simulations, made by considering a uniform medium (Fig. 4).

The intensity of the 1st order of diffraction obtained with LC-cells, in both polarizations (green and orange points in Fig. 4), are comparable to those obtained with reference-index liquid-cells and RCWA simulations. It can thus be considered that the liquid crystals are perfectly aligned inside the diffraction gratings. This assertion is confirmed by the characterization of cells between crossed polarizers (Fig. 5), allowing to observe a perfect extinction at the diffraction grating level.
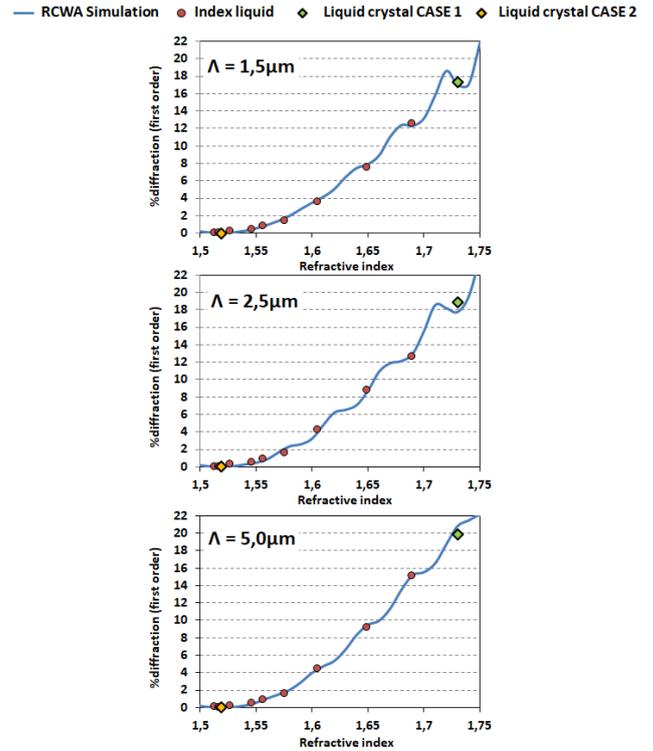

Fig. 4. First-order diffraction measurements on cells with 840nm depth gratings impregnated with various index liquids (red circles), liquid crystals in S or P-polarizations (green or yellow diamonds) compared to RCWA simulations (blue curve).

Finally, a 90° rotation from S to P polarization (i.e. CASE1 to CASE2) turns off the diffraction by more than 99.8%. The residual diffraction results from an uncertainty in the refractive index of LCs and resins estimated at 5.10^{-3}.
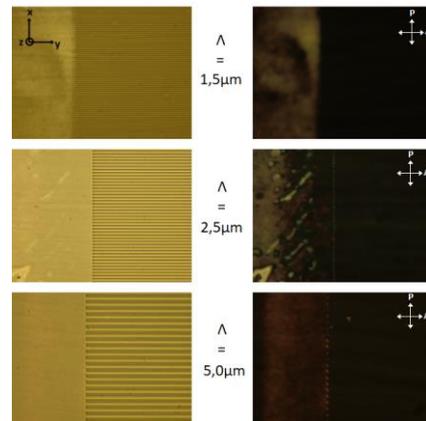

Fig. 5. Optical microscopy observation (x50) of LC-impregnated diffraction gratings with period from 1.5 to 5.0μm and 840nm depth without polarizers (in left) and between cross polarizers (in right). As expected for aligned LCs, transmission is extinguished between crossed polarizers.

3.2 Application of tension with S-polarized incident light (CASE1 to CASE3)

We confirmed that in the passive state (no voltage) the LCs are effectively aligned in gratings. We then focused on the effect of an electric field on the diffraction of a S-polarized incident light (switching from CASE1 to CASE3 in Fig. 3). The application of a voltage has been performed on LC-impregnated cells to study the movement of liquid crystals, relating to the extinction of the diffraction. Fig. 6 shows diffraction measurements with applied voltage for various grating periods and for two different grating depths (respectively 120 and 840nm in the upper and the lower part).
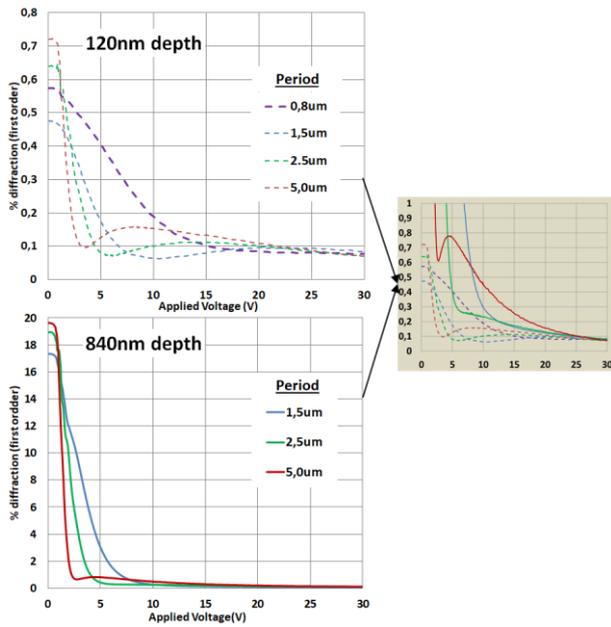

Fig. 6. Characterization of first order diffraction of LC-impregnated cells illuminated with a S-polarized incident beam depending of the applied electric field for various grating periods (purple to red lines) at depths of 120 (dashed lines on the top) or 840nm (plain curves below). Inset: comparison for all periods and depths to show the maximal extinction of diffraction occurs at the same level ($\approx$0.1%).

The diffraction percentage drops first very fast at low voltage before being quasi-constant at higher voltage. The decrease of the observed diffraction allows validating the mobility of the molecules in grooves from 2.5µm down to 0.4µm widths. These dimensions are adapted to the use of a GMRF in the near-IR range.

However, the applied voltage needed to turn off the diffraction is higher when the period is reduced. Indeed, considering the first low-voltage diffraction drop of 840nm depth gratings, a slope of $14.6V^{-1}$ is measured for 5µm period for only $5.8V^{-1}$ for a 2.5µm grating, or even $2.9V^{-1}$ for a period of 1.5µm. We can infer a reduction of the mobility of the LC molecules when confined in narrower structures. A reduction in the period increases the specific surface area and therefore the proportion of LC / resin interfaces restricting the movement of the molecules under electric field.

From a voltage higher than 20V, the diffraction is the same whatever the depth and the period. The value of the residual diffraction ($\approx$ 0.1% diffraction to 20V) is one order of magnitude higher than that obtained in the CASE2 ($\approx$ 0.01% diffraction). Thus, liquid crystals must not be perfectly in a homeotropic alignment in the grating, even at high voltage. Finally, 99% of the initial diffraction is turned off for 840nm-deep gratings against 90% for 120nm-deep ones.

The residual diffraction probably results from an anchoring layer (also called extrapolation length or Fréedericksz transition (Freedericksz and Zolina 1933)), that is a portion of molecules misaligned at the surface preventing the refractive index from being totally matched with the structure. Since the residual diffraction is the same regardless of diffraction grating depth, the anchoring layer is assumed to be situated effective only on horizontal surfaces. The anchoring layer is therefore considered negligible on the vertical flanks.

3.3 Application of tension with P-polarized incident light (CASE2 to CASE4)

In P-polarization, the LC-impregnated grating is supposed to be non-diffractive with or without tension (Fig. 3). However, the passage through a diffractive shape between CASE2 and CASE4 is observed (Fig. 7).
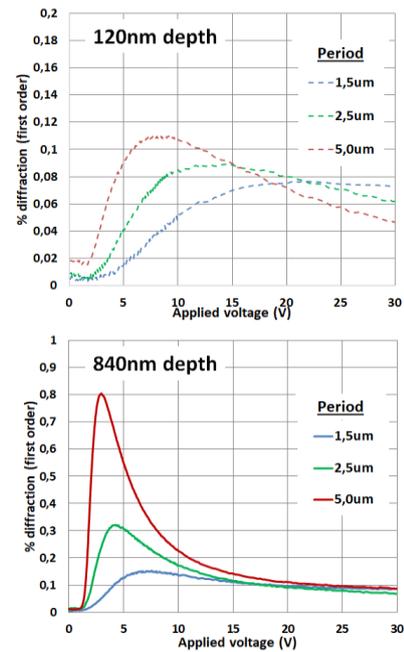

Fig. 7. Characterization of first order diffraction of LC-impregnated cells illuminated with a P-polarized incident beam depending of the applied electric field for various grating periods (purple to red lines) at depths of 120 (dashed lines on the top) or 840nm (plain curves below).

The formation of an inhomogeneous electric field, by the difference of permittivity between the structure and the liquid crystals, can explain the diffraction variations. Indeed, the variation of electric field will generate a vertical offset of the equipotential between the teeth and grooves of the grating. If the field lines are considered vertical in the center of the areas concerned, this is not the case near teeth/grooves interfaces, where the field is oriented in the plane (x, z). This assumption is confirmed by the appearance of birefringence zones in these areas when the cell is observed, under tension, between crossed polarizers (Fig. 8).
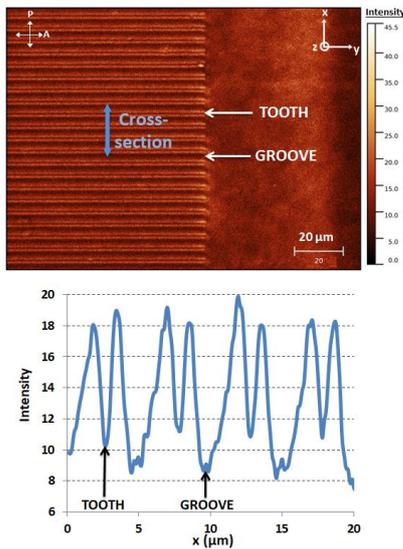

Fig. 8. Microscopic observation (x50) between cross polarizers of LC-impregnated diffraction gratings (5.0µm period and 840nm depth) with a tension of 10V applied in the cell (at the top). A cross section show the repartition of the birefringence in teeth/groove interfaces (below).

4 Characterization with white light : visible diffraction spectra

In order to study the evolution of the diffraction as a function of the wavelength in the different cases, a characterization with white light was carried out.

A white light source is placed in normal incidence relative to the sample, both being placed on a rotating support. The white light is decomposed by the grating, each wavelength being diffracted at a particular angle. The diffracted signal is then directed to a spectrometer to measure its intensity according to the wavelength. The rotary support makes it possible to modify the angle of detection, providing the spectrum of diffraction efficiency of the studied grating over the entire visible range (Fig. 9).
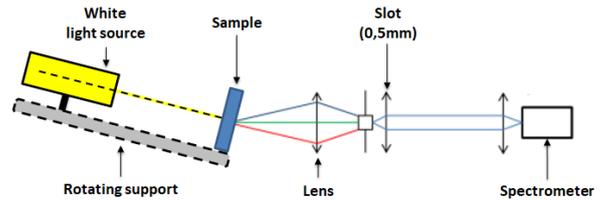

Fig. 9. Schematic view of the characterization bench for measuring the diffraction efficiency at different wavelengths

The results presented are obtained with a 1.5µm grating period and 840nm deep, a sample made by photolithography.

4.1 Modulation of incident polarization without tension (comparison of CASE1 and CASE2)

The both zero-voltage diffraction case are first characterized with an incident wave in polarization S (CASE1, diffractive) and P (CASE2, non-diffractive) for wavelengths between 500 and 800nm (Fig. 10). Each Gaussian curve represents a diffracted wavelength measured at a certain angle and the whole is obtained by rotating the rotary support by a few degrees. The thick red curve represents the diffraction spectrum associated with these measurements.
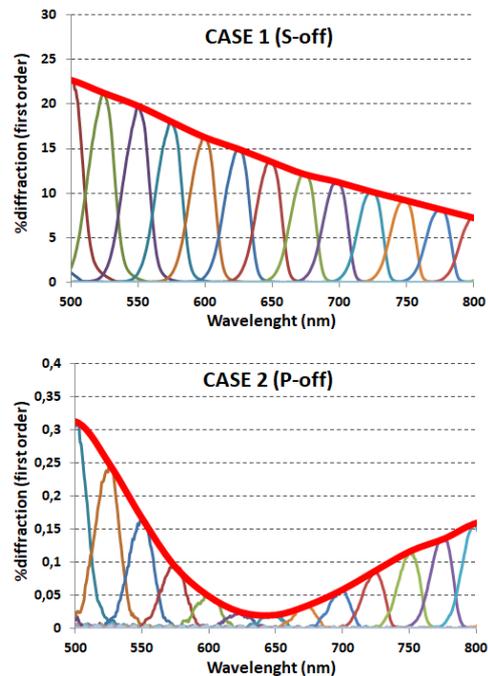

Fig.10. First order's diffraction spectrum (in red, bold) obtained as the envelope of the experimental measurements at different diffraction angles (fine colors). LC-impregnated grating with 1.5µm period and 840nm deep is illuminated with a S-polarized incident beam (at the top) and P-polarized light (bottom) without applied voltage.

In the CASE 1, a progressive decrease from 22,7% at 500nm to 7.2% at 800nm is observed. For the CASE 2, the diffraction spectrum passes through a minimum 0.012% at

635nm. The diffraction remains relatively low with maximums of 0.31% at 500 nm and 0.16% at 800 nm.

The shape of these diffraction spectra is perfectly explained when compared to the evolution of $|\Delta n|$; difference between the resin refractive index (n_{ulis}) and the CL's refractive index (n_o or n_e); as a function of the wavelength (Fig. 11).
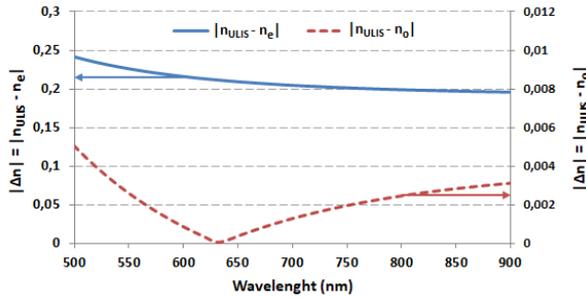

Fig.11. Difference between the ULIS resin refractive index and liquid crystal E7 considering extraordinary index (blue plain line, left Y axis) and ordinary index (red dashed line, right Y axis). Refractive index of ULIS resin was measured by ellipsometry while E7 liquid crystal dispersion curves are derived from extended experimental measurements by a three-coefficient Cauchy model (Li and al. 2005).

Indeed, the forms of $n_{ulis}-n_e$ and $n_{ulis}-n_o$ are closely linked with the diffraction spectra obtained respectively in polarization S and in polarization P. A decay is observed in the first case and a minimum at 635nm (when the curves of dispersion intersect) in the second one.

4.2 Application of tension with S-polarized incident light (CASE3)

Finally, diffraction spectra of LC-cell (1.5µm period and 840nm deep) with different applied voltages (U=4, 10 or 30V) are measured with S-polarized incident beam (Fig.12).

For a voltage of 4 or 10V, the shape of the curve is similar to the one obtained in S-polarization with a no-voltage cell, corresponding to the index difference between the resin and the LC's extraordinary index. For a voltage of 30V, there is nevertheless a minimum between 600 and 700 nm, recalling the shape of the difference between the n_{ulis} and n_o.

It would therefore seem that the CL index perceived by the light wave is still predominantly the extraordinary index for voltages of 4 or 10V. On the other hand, the ordinary index becomes more influential for a voltage of thirty volts.
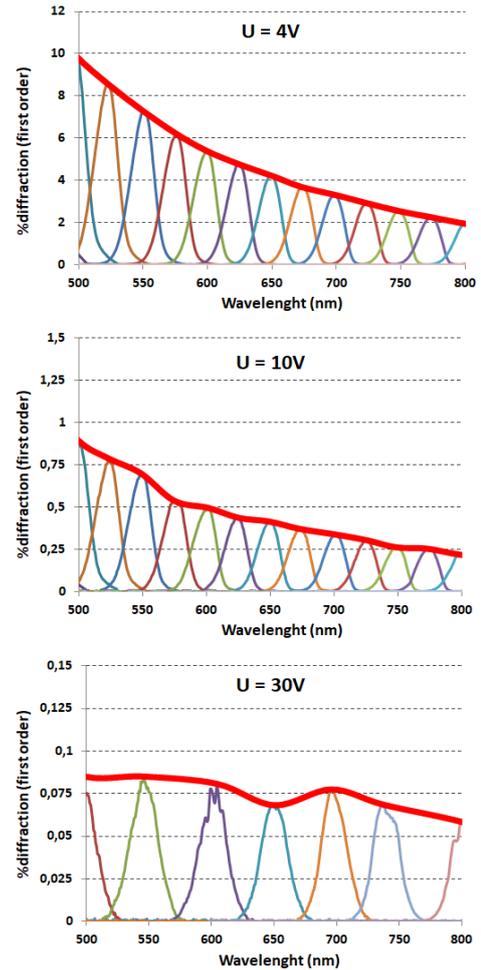

Fig.12. First order diffraction spectrum (in red, bold) obtained as the envelope of the experimental measurements at different diffraction angles (fine colors). LC-impregnated grating with 1.5µm period and 840nm deep is illuminated with a S-polarized incident beam and various applied voltages: 4V (above), 10V (middle), 30V (bottom).

5 Conclusion

In this work, we have demonstrated the possibility of switching liquid crystals inside sub-micrometric structures, leading to switch the diffractive state from ON to OFF. Without voltage, the alignment of molecules in gratings seems almost perfect and their mobility under electric field is proven down to 400nm-width grooves. These dimensions are adapted to the use of a GMRF in the near-IR range. Total extinction of diffraction seems to be weakened by horizontals anchoring layers which are always present for a voltage beyond 30V.

However, it is possible to use the same principle with a non-diffractive shape without voltage to benefit from optimized extinction due to near-perfect alignment of liquid crystals in the structure. In order to do so, one can for example use a structure with a refractive index close to the extraordinary index of liquid crystals.

The fact that the vertical anchoring layers are negligible should allow this principle to be applied for smaller periods, even if the diffraction drop depending to the voltage will be slower. However, with a reduction of grating depth (<50nm), the effect should be drastically weakened by horizontal anchoring layers.

A reduction of the cell thickness (7µm in our experiments) should reduce the voltage to be applied to modulate the diffraction.

References

Alonso-Ramos C, Zavargo-Peche L, Ortega-Moñux A, Halir R, Molina-Fernández I, Cheben P (2012) Polarization-independent grating coupler for micrometric silicon rib waveguides. Opt Letter 37(17):3663-3665

Biver C, Deliane F, Etienne P, Llosa M, Cano JP, Ballet J (2009) Method for preparing a photocrosslinkable composition. Patent EP2262848A1

Caputo R, De Sio L, Veltri A, Umeton C, Sukhov AV (2004) Development of a new kind of switchable holographic grating made of liquid-crystal films separated by slices of polymeric material. Opt express, 29(11):1261-1263

Chang ASP, Tan H, Bai S, Wu H, Yu Z, Chou SY (2007) Tunable Liquid Crystal-Resonant Grating Filter Fabricated by Nanoimprint Lithography. IEEE Photon Technol Lett, 19(19):1457-1459

Chen H, Tan G, Huang Y, Weng Y, Choi T, Yoon T, Wu S (2017) A Low Voltage Liquid Crystal Phase Grating with Switchable Diffraction Angles. Nature 7:39923

Doucet JB, and al. (2016) Transfert de nanostructures dans la silice par nanoimpression avec résines 'maison'. Presented at the Journées Nano, Micro et Optoélectronique, Les Issambres, France.

Freedericksz V, Zolina V (1933) Forces causing the orientation of an anisotropic liquid. Transactions of the Faraday Society, 29:919–930

Gao L, Zheng Z, Zhu J, Han W, Sun Y (2016) Dual-period tunable phase grating based on a single in-plane switching. Opt Letter, 41(16):3775-3778

Hu W, Srivastava A, Xu F, Sun J, Lin X, Cui H, Chigrinov V, Lu Y (2012) Liquid crystal gratings based on alternate TN and PA photoalignment. Opt Express, 20(5):5385-5391

Kapoustine V, Kazakevitch A, So V, Tam R (2006) Simple method of formation of switchable liquid crystal gratings by introducing periodic photoalignment pattern into liquid crystal cell. Opt Communications, 266(1):1-5

Li J, Wu S, Brugioni S, Meucci R, Faetti S (2005) Infrared refractive indices of liquid crystals. Journal of Applied Physics. 97(7):073501

Lindquist RG, Leslie TM, Kulick JH, Nordin GP, Jarem JM, Kowel ST, Friends M (1994) High-resolution liquid-crystal phase grating formed by fringing fields from interdigitated electrodes. Opt Lett, 19(9):670-672

Lu X, Lee FK, Sheng P, Kwok HS, Chigrinov VG, Tsui OKC (2006) Substrate patterning for liquid crystal alignment by optical interference. Appl Phys Lett, 88(24):350-358

Margerum JD, Lackner AM, Smith GW, Vaz N, Kohler JL, Allison CR (1992) Polymer dispersed liquid crystal film devices. Patent US5096282A

Pavani K, Naydenova I, Raghavendra J, Martin S, Toal V (2009) Electro-optical switching of the holographic polymer-dispersed liquid crystal diffraction gratings. Journal of Optics A: Pure and Applied Optics, 11(2):23-24

Pelloquin S, Augé S, Sharshavina K, Doucet JB, Héliot A, Camon H, Gauthier-Lafaye O (2018) Soft mold NanoImprint Lithography: a versatile tool for sub-wavelength grating applications. Microsyst Technol, 1-8.

Sharon A, Rosenblatt D, Friesem AA, Weber HG, Engel H, Steingrueber R (1996) Light modulation with resonant grating–waveguide structures. Opt Lett, 21(19):1564-1566.

Taillaert D, Bogaerts W, Bienstman P, Krauss TF, Van Daele P, Moerman I, Verstuyft S, De Mesel K, Baets R (2002) An out-of-plane grating coupler for efficient butt-coupling between compact planar waveguides and single-mode fibers. IEEE J. Quantum Electron, 38(7):949-955

Wang C, Hou H, Chang P, Li C, Jau H, Hung Y, Lin T (2013) Full-color reflectance-tunable filter based on liquid crystal cladded guided-mode resonant grating. Opt Express 245(20):22892-22898

Wang SS, Magnusson R (1993) Theory and applications of guided-mode resonance filters. Appl Opt, 32(14):2606-2613

Wen B, Petschek RG, Rosenblatt C (2002) Nematic liquid-crystal polarization gratings by modification of surface alignment. Appl Opt, 41(7):1246–1250

Zheng J, Ge C, Wagner CJ, Lu M, Cunningham BT, Hewitt JD, Eden JG (2012) Tunable ring laser with internal injection seeding and an optically-driven photonic crystal reflector. Opt Express, 19(14):14292-14301